Mol. Cells *34*, 481-493, November 30, 2012
DOI/10.1007/s10059-012-0246-4
pISSN: 1016-8478 eISSN: 0219-1032

Molecules and Cells
http://molcells.org

Thymic Epithelial Requirement for γδ T Cell Development Revealed in the Cell Ablation Transgenic System with *TSCOT* Promoter

Gwanghee Lee[1,3], Ki Yeon Kim, Cheong-Hee Chang[2], and Moon Gyo Kim*

In order to investigate the role of thymic epithelial cell (TEC) subsets during T-cell development, we established a new transgenic system, enabling inducible cell-specific ablation as well as marking the TEC subsets using bicistronic bacterial *nitroreductase* and *EGFP* genes. Two different lengths of the *TSCOT* promoter in transgenic mice, named 3.1T-NE and 9.1T-NE, drive EGFP expression into TECs. In adult life, EGFP expression was located in the medulla with a smaller 3.1 kb *TSCOT* promoter, while it was maintained in the cortex with a 9.1 kb promoter, suggesting putative TEC specific as well as compartment specific cis elements within two promoters. Nitroreductase induced cell death was specific without bystander killing upon the treatment of prodrugs such as nitrofurantoin and metronidazol. The degree of cell death was dependent on the dose of the prodrug in the cell and the fetal thymic organ cultures (FTOCs). Fetal thymic stromal populations were analyzed based on the expression levels of EpCAM, MHCII, CDR1 and/or UEA-1. EGFP expression patterns varied among subsets indicating the differential *TSCOT* promoter activity in each TEC subset. Prodrug treatment in FTOCs reduced the numbers of total and subsets of thymocytes. A $CD4^+CD8^+$ double positive cell population was highly susceptible in both transgenic lines. Surprisingly, there was a distinct reduction in γδ T cell population only in the 9.1T-NE thymus, indicating that they require a NTR-EGFP expressing TEC population. Therefore, these results support a division of labor within TEC subsets for the αβ and γδ lineage specification.

INTRODUCTION

Thymic organogenesis in mice begins around fetal day 11 by forming of an initial thymic epithelial rudiment that continues to develop further through postnatal stages until puberty (Blackburn and Manley, 2004). Thymic stromal cells that constitute a major part of the microenvironment include thymic epithelial cells (TECs), fibroblasts, and hematopoietically-derived dendritic cells and macrophages. They develop within the thymus and support complex thymic differentiation processes including αβ and γδT cell lineage specification, selection as well as migration (Anderson and Takahama, 2012; Anderson et al., 2009; Petrie, 2003; Petrie and Zuniga-Pflucker, 2007; Rodewald, 2008).

It is currently well understood that, among the stromal cells, TECs play a major role in thymic organogenesis as well as in the positive and the negative selection of thymocytes (Ladi et al., 2006; Takahama, 2006). In an adult thymus, the microenvironment is separated into different structural compartments; the subcapsule, cortex, medulla, and the corticomedullary junction. Migration of developing thymocytes in the thymic microenvironment is also critically important for the survival and selection of developing thymocytes (Takahama, 2006; Takahama et al., 2010). While these different compartments are thought to be involved in particular aspects of thymic functions, their precise roles are not fully understood. During the early fetal phase of thymic development, the thymic microenvironment is also undergoing development. Developmental processes of two major lineages, cortical TEC (cTEC) and medullary TEC (mTEC) from the single stem cells are well established (Roberts et al., 2012), however, the compartmentalization process is still under active investigation. Although major compartment specific TEC surface markers such as EpCAM, MHCII, CDR1 and UEA-1 are easily detectible (Shakib et al., 2009; Yang et al., 2005), their profiles specific to developmental stages and lineages need to be further established.

The development of fetal thymocytes is different from that of their adult counterpart in terms of kinetics and spatial distribution. The traffic pattern of fetal thymocytes is also suggested to be different from that of a mature thymus since compartmentalization is not yet complete and the blood vessel system has not been established in fetal stages. During fetal development, particular thymocyte lineages and subsets appear in waves, and there are clear biases in the relative abundance of γδ T cells and early αβ T cells (double negative, DN for CD4 and

Department of Biological Sciences, Inha University, Incheon 402-701, Korea, [1]Department of Cell Biology and Physiology, Washington University School of Medicine, St Louis, MO 63110, USA, [2]Department of Microbiology and Immunology, The University of Michigan Medical School, Ann Arbor, MI 48109-0620, USA, [3]Present address: Department of Physiological Chemistry, Genentech, South San Francisco, CA 94080, USA
*Correspondence: mgkim@inha.ac.kr

Received September 14, 2012; accepted October 10, 2012; published online November 15, 2012

Keywords: EGFP, fetal thymic organ culture, gamma delta T cell, thymic epithelial cell, transgenic mouse

CD8) in the fetal thymus while these cells are rare in proportion, and therefore, difficult to follow in the adult thymus. The repertoires of γδ T cells in the fetal thymus are also unique (Cahill et al., 1999; Jenkinson and Owen, 1990). (Vγ5) γδ T cells appear in the thymus only during the fetal stage and migrate later into the different peripheral epithelial tissues. Therefore, it is ideal to take an advantage of fetal thymic organ cultures (FTOCs) (Anderson and Jenkinson, 2007; Anderson et al., 1993; Jenkinson and Anderson, 1994) or reaggregate thymic organ cultures (RTOC) (Anderson et al., 1993; White et al., 2008) *in vitro* for the detailed study of interactions between early developing thymocytes and the thymic microenvironment.

The choice between different lineages of thymocytes is the result of molecular interactions between thymic stromal cells and developing thymocytes (Ciofani and Zuniga-Pflucker, 2010; Crompton et al., 2007; Laky and Fowlkes, 2008; Laky et al., 2006; Narayan and Kang, 2007; Wong and Zuniga-Pflucker, 2010). From studies on genetically modified mouse lines, molecules such as sonic hedgehog homolog, wnt, notch, and their ligands were suggested in playing roles for the decision of T cell lineage commitment, αβ vs. γδ T cells, CD4 vs. CD8. In addition, NFκB signaling is important in the development and the cross talk of (Vγ5) γδ T cells and AIRE$^+$ mTEC (Roberts et al., 2012). However, the mechanisms of cellular and molecular actions between TEC and thymocytes still are not clearly understood for the most part. It is still an important question as to which specific TEC subsets take part in the choice and progression of thymocyte lineages. However, it is challenging to answer this question because of the multilevel complexities and difficulties associated with the purification of less abundant TEC. Recently, using fetal thymuses from genetically modified mouse systems, the importance of RANK signaling was identified for the development of invariant (Vγ5) γδ T cells and Aire$^+$ medullary epithelium (Roberts et al., 2012). This report provided the critical evidence for the Aire$^+$ epithelium dependent upon (Vγ5) γδ T cells as well as those required for (Vγ5) γδ T cell development. In addition, the Aire$^+$ epithelial cells were located in the medullary islets of the fetal thymus. It remains to be determined whether the Aire$^+$ epithelial cells at fetal stages exhibit the properties of mature mTEC or precursor cells since TEC stem cells are found in the medullary islets in young mice.

The analysis of TEC compartments solely depending on immunohistology can mislead the interpretation on the expression of specific markers since cortical staining is difficult with many antibodies (Yang et al., 2006). The results of flow cytometry with isolated TEC preparation may be unintentionally different and purified TEC populations may easily be contaminated with other types of TEC populations. Cell surface markers so far useful for separating TEC compartments are EpCAM and MHCII for all TEC, CDR1 and CD205 for cTEC, UEA-1 for mTEC (Gray et al., 2002; 2006; Shakib et al., 2009 Yang et al., 2006). Intracellular markers considered useful are keratin 5 and B5t for cTEC and Keratin 8, AIRE and MTS10 for mTEC. In addition to expression itself, the organization of molecules can be compartment specific. For example, MHCII molecules in the cortical but not in the medullary thymic compartment form aggregates as we described (Yang et al., 2006).

Thymic stromal cotransporter (TSCOT) is a gene originally identified from a fetal thymic stromal cDNA library (Jo et al., 2001; Lee et al., 1998; 2001; Park, 1997) and was assigned as a cTEC marker, Ly110 (Ahn et al., 2008; Kim et al., 1998; 2000a; Yang et al., 2005). Using its interesting limited gene expression pattern, we previously tested a hypothesis if the thymic compartment for the negative selection is exclusively allocated to the medulla (Laufer et al., 1996; 1999). When the *LacZ* gene is targeted into the *TSCOT* locus, specific CD4 tolerance to the cortical β-galactosidase antigen was efficiently established with the high sensitivity without cross presentation, supporting the idea that there is no exclusion in the cortical TEC compartments for the removal of self-reactive T cells (Ahn et al., 2008; Laufer, 2008).

Here, we report a study on the role of TEC subsets for thymocyte development by using a new mouse model that can undergo specific TEC ablation. Ablation was achieved by using the transgene comprised of the *TSCOT* promoter, the reporter *EGFP*, and a suicide gene *nitroreductase* (*NTR*). Two different lengths of the *TSCOT* promoter directed the expression of EGFP and NTR to different TEC compartments with some overlap, which resulted in ablation of differential subsets of TEC. Interestingly, experiments using FTOCs and RTOCs in conjunction with TEC ablation showed the segregation of fetal αβ and γδ T lineage commitment in addition to early thymocyte differentiation, suggesting a distinct role of specific TEC subsets during T cell development.

MATERIALS AND METHODS

Chemicals

Prodrugs, nitrofurantoin [N-(5-nitro-2-furfurylidene)-1-aminohydantoin] (NFT) and metronidazole (2-methyl-5-nitroimidazole-1-ethanol) (MTZ) for inducing NTR specific cell ablation were purchased from Sigma.

Mice and cells

Transgenic mouse lines were generated in the transgenic facilities at NCI (Dr. Lionel Fagenbaum) and NIAID transgenic facilities (Dr. Judy Hewitt) in NIH and then transferred to the Samsung Animal Facility at Sungkyunkwan University (Dr. Han-Woong Lee), and maintained in the Laboratory of Molecular and Cellular Immunology Animal Facility of Inha University, Korea. Transgenes, p3.1T-NE and p9.1T-NE, were constructed using 3.1 kb and 9.1 kb fragments of the *TSCOT* promoter (Chen et al., 2000) with pCMV-NTR-IRES-EGFP derived from the *NTR* gene from pNR3 (a kind gift from Dr. Shuhei Zenno, University of Kyoto) and pIRES2EGFP (Clontech). All animal studies are in compliance with the Use of Laboratory Animals under the proper protocols. The protocols were approved by the Committees on the Ethics of Animal Experiments of NIH (LCMI Protocol 8), Sungkyunkwan University (Protocol HWL/MGK-1), and Inha University (Protocol LMCI-2). Fetal mice were obtained from timed mating. A presence of a vaginal plug was considered at E0.5.

For genotyping, tail samples were extracted and used for polymerase chain reaction with primers for the *NTR* locus, PNR3-R (TGATGACGGCTGAAACAGGG) and PNR3-F (TGA ACCTTGATAATCTGCTGGCAG) and primers for *EGFP* locus: EGFP-F (GCCACAAGTTCAGCGTGTCC), EGFP-R (GCTTCT GTTGGGGTCTTTGC), using the red Extract-N-Amp Tissue PCR kit (Sigma).

NIH3T3 and 293T cells were grown in DMEM with 5% bovine calf serum and 10% fetal bovine serum (FBS), respectively, and transfected with a DNA/$CaCl_2$ solution. Thymocyte suspensions were prepared by filtration through a nylon mesh. Thymic epithelial cells were collected from the cultures of fetal thymus with 1.35 mM 2-deoxyguanosine (2d-Guo) in the 6-well transwell plate (Corning Incorporated) in the presence and absence of prodrugs. A single cell suspension was prepared by digestion with 0.25% trypsin (Invitrogen) for about 20 min, in the

presence of DNase I (Sigma) if needed, and washed with phosphate buffered saline (PBS) containing 10% FBS. For further purification of TEC, the single cell suspension was isolated using magnetic bead cell sorting after incubating with anti-Fc mAb 2.4G2 and anti-mouse CD45 microbeads (Milteny Biotec) for 20 min at 4°C.

Apoptosis assay

HEK293T cells were transfected with 10 μg of pCMV-NTR-EGFP or pEGFP-N1 with the $CaPO_4$ method. After one day, cells were photographed in order to count the EGFP expressing cells under the fluorescent phase contrast microscope (Olympus IX71) using AxioVision AC Rel. 4.5, and divided into groups for the drug treatment. For annexin V staining, 1×10^5 cells were pelleted on a 96-well U-Bottom plate and stained with biotin-conjugated Annexin V (BD Pharmingen) in Annexin V binding buffer (BD Pharmingen). After washing, APC-conjugated streptavidin (BD Pharmingen) was added, and analyzed by using a flow cytometer (BD FACSCalibur) and Flowjo v8.7.

Antibodies and flow cytometry

Monoclonal antibodies used in the staining of cells were anti-CD4 (L3T4 or RM405), anti-CD8 (Ly-2), anti-MHCII (I-A^b), anti-γδTCR (GL3), anti-CD44 (Ly24), anti-CD45 (Ly-5) and anti-CD25 (Il-2R). The antibodies were purchased from Caltag or from BD PharMingen. Anti-aminopeptidase A (CDR-1) and anti-EpCAM (G8.8) were purchased from American Type Culture Collection and were prepared by Dr. Larry Lantz in the Custom Antibody Services Facility, NIAID, NIH. Biotinylated UEA-1 was purchased from Vector Laboratories.

Cells were washed in cold FACS buffer (PBS + 1% BSA), and subsequently stained on ice with the primary and the secondary antibodies, then analyzed on a FACSCalibur or FACSAria with two lasers in the presence of 1-2 μg/ml of propidium iodide (PI). Anti-Fc, 2.4G2 antibody was included in all flow cytometry staining as an Fc block. Analyses were done using the FlowJo program.

Microscopy

For the detection of EGFP in newborn transgenic mice, a stereomicroscope (Olympus SZXP) was used. The presence of autofluorescence was verified by the red signal without any staining. For the detection of EGFP from the thymic sections, confocal microscopy was performed on the frozen sections in the NIAID confocal facility (Leica SP2) with help from Dr. Owen M. Schwartz. For the enzymatic detection of NTR, red-shifted substrate, a CytoCy5S (emission 638nm, GE healthcare) was used. Briefly, cells were treated with 1 μM CytoCy5S in serum free media for 2 h, washed twice with PBS, and analyzed by phase contrast inverted fluorescence microscopy (IX71; Olympus) equipped with a mercury lamp. Green (excitation; 460-490 nm, emission; 520 nm~) and red (excitation; 510-550, emission ; 590 nm~) filters were used.

FTOC and RTOC

For FTOC, fetal thymic lobes were collected from 14.5 day old embryos, and cultured with Iscove's Modified Dulbecco's Medium (IMDM) containing 10% FBS on 6-well transwell plates. Each group contained at least 14 thymic lobes. After being cultured for designated days, thymocytes were recovered and analyzed using flow cytometry. For thymic epithelial cell analysis, E14.5 fetal thymic lobes were cultured with FTOC media containing 1.35 mM 2d-Guo in the presence and absence of 30 μM prodrugs in DMSO. Untreated samples contained the same concentration of DMSO. For RTOC, the thymic stromal cells were prepared by treating E14.5 fetal thymus samples with 2-dGuo with and without prodrugs. Fetal liver progenitor cells from C57BL/6 mice were reaggregated with the prepared stromal cells. Recovered cells were counted and then analyzed by flow cytometry after 7-14 days of culture in a humidified chamber.

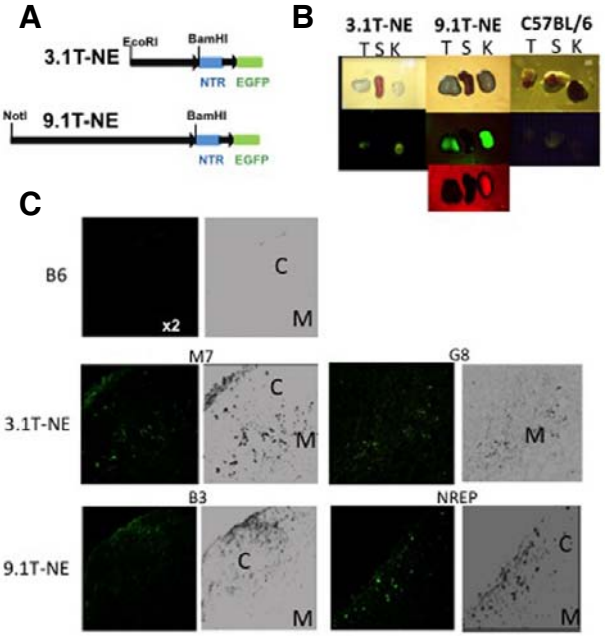

Fig. 1. Transgenic mouse lines with TEC targeted expression of NTR-IRES-EGFP. (A) Construct used for the generation of transgenic mouse. 3.1 kb of the *TSCOT* promoter was used in 3.1T-NE and 9.1 kb of the *TSCOT* promoter in 9.1T-NE, respectively. (B) Thymic expression of EGFP in new born 3.1T-NE and 9.1T-NE transgenic mice and C57BL/6 (Magnification at 5×). Kidney (K), spleen (S), thymus (T). The presence of autofluorescence in the kidney sample is apparent with the red fluorescence without staining. (C) Compartmentalized activity of 3.1 kb and 9.1 kb promoters in adult NTR-IRES-EGFP transgenic mice. EGFP expression in confocal microscopy (magnification at 200×) of normal nontransgenic thymus from C57BL/6 (B6), thymuses of 3.1T-NE (M7 and G8), 9.1T-NE (B3 and NREP) are shown on the left. Stylized patterns (converting image to grayscale, and "find edges" in the stylize filter of Photoshop 10.0) of images are shown on the right for better visual presentation.

RESULTS

The 3.1 kb and 9.1 kb *TSCOT* promoters drive compartment specific expression of EGFP

To study the role of TEC subsets for thymocyte development, we generated an inducible TEC ablation system. For this purpose, we used two different lengths of the TEC specific *TSCOT* promoter to direct the bicistronic expression of *EGFP* and NTR for monitering the transgene expression and for inducing cell death, respectively (Fig. 1A).

Transgenic mice expressing the 3.1 kb (3.1T-NE) or 9.1 kb fragment (9.1T-NE) containing additional 6 kb upstream sequences were able to express bicistronic *NTR-IRES-EGFP* in

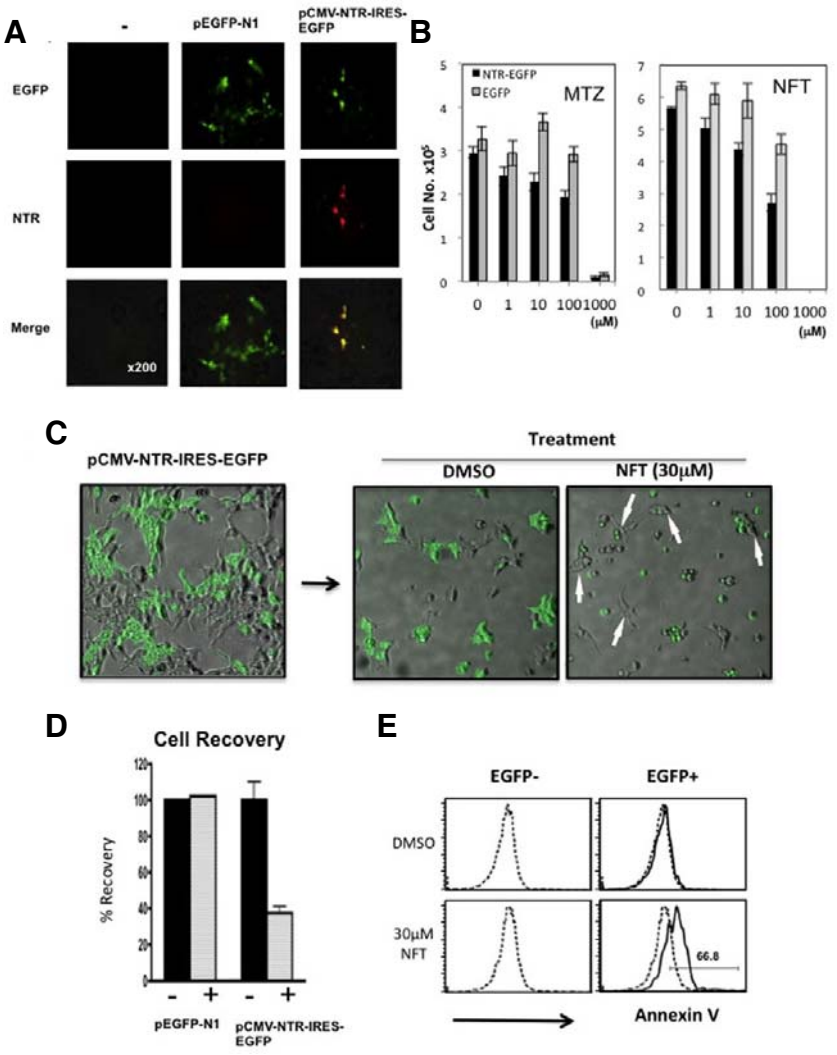

Fig. 2. Evaluation of prodrugs, MTZ and NFT for NTR mediated apoptosis in cell culture. (A) NIH3T3 cells transfected with pEGFP-N1 or pCMV-NTR-IRES-EGFP constructs. NTR enzymatic activity was tested using cytocy5S under fluorescent phase contrast microscope in the red channel. EGFP expressing green cells are also red in the pCMV-NTR-IRES-EGFP transfected group. (B) Dose response of MTZ and NFT prodrugs in NIH3T3 cell pools stably transfected with pEGFP-N1 or pCMV-NTR-IRES-EGFP. Cells were counted after treating with prodrugs for 3 days. (C) Minimal bystander killing of NTR nonexpressor by prodrug treatments to HEK293T cells transiently transfected with pCMV-NTR-IRES-EGFP. One day after transfection, cells were divided and treated with DMSO or NFT. Cells observed 1 day after treatment of prodrugs. Normal shaped cells attached with $EGFP^+$ dying cells are indicated with arrows. (D) The relative recoveries of HEK293T cells transfected with pEGFP-N1 or pCMV-NTR-IRES-EGFP after treatment with DMSO (-) or NFT (30 μM) (+). (E) Representative annexin V staining profiles of transiently pCMV-NTR-IRES-EGFP transfected HEK293T cells after treatment. Annexin V^+ population was seen only in NFT treated $EGFP^+$ cells. Histograms shown are from the PI negative gates.

the thymus. As seen in Fig. 1B, both transgenic lines showed green fluorescence in the thymus and kidney but not in the spleen or other tissues when tested at newborn stages (Fig. 1B and data not shown). The signals in the newborn kidneys were likely due to a high level of autofluorescence seen as a strong signal in red channels. Nontransgenic thymuses from C57BL/6 mice showed little autofluorescence (Fig. 1B and data not shown).

When adult thymuses were tested for EGFP expression, two founder lines of 3.1T-NE lines (M7 and G8) showed the expression in the medulla and the corticomedullary junction (CMJ) (Fig. 1C and data not shown). In contrast, 9.1T-NE founder lines (B3 and NREP) showed a more limited expression in the cortical area (Fig. 1C and data not shown). No signal was detected in the thymus from C57BL/6 mice. In addition, there was no sign of EGFP expression in any of the thymocytes (data not shown). Based on these results, we concluded that the expression of the transgene is compartment specific due to the difference in the regulatory elements in each length of the promoter.

Specificity of NTR-mediated apoptotic cell death without significant bystander killing

Having established the expression pattern of two transgenes, we tested the inducible cell ablation using NTR. To do this, we chose to test less conventional prodrugs, MTZ and NFT, instead of more commonly used CB1954 (Bailey and Hart, 1997) since they are more readily available from commercial sources. MTZ and NFT were previously evaluated as useful candidates as NTR prodrugs (Bridgewater et al., 1997). In addition, CB1954 was reported to show bystander killing through cell permeable metabolites (Bailey et al., 1996).

To test the killing effect *in vitro* first, we introduced NIH3T3 cells with a construct that expresses *NTR* and *EGFP* by the CMV promoter, pCMV-NTR-IRES-EGFP. As a control, pEGFP-N1 which does not have the *NTR* gene, was used. As shown in Fig. 2A, EGFP expressing cells showed the NTR activity (red fluorescence) when pCMV-NTR-IRES-EGFP was introduced into the cell. Next, the effect of prodrugs was examined by comparing cell survival after treating cells for 3 days with prodrugs (Fig. 2B). The result showed that both MTZ and NFT treatments revealed dose dependent decreases in the number of cells expressing NTR but not the control (pEGFP-N1 transfected) up to 10 μM concentrations of prodrugs. However, a concentration of MTZ and NFT higher than 100 μM showed NTR-independent killing of the cells although the killing effects

Table 1. Analysis of apoptosis on the HEK 293T cells transfected with pCMV-NTR-EGFP after treatment with NFT

Treatment	EGFP-	EGFP+
DMSO	42.23 ± 2.224	45.13 ± 1.241^{ns}
NFT 30 μM	51.9 ± 0.907	109.67 ± 2.848***

Mean fluorescence intensity (MFI) and standard error of means (SE) are taken from the values of Annexin V stain in flow cytometric analyses.
***P < 0.0001 between EGFP- and EGFP+ in NFT treated cells, ns: non-significant. P values are tested by Two-tailed unpaired *T*-test in Prism 4.

(NTR$^+$/NTR$^-$) was better (data not shown). At 1,000 μM, nearly all the cells did not survive. From these results, we chose to use 30 μM for the subsequent experiments.

Next, we tested whether cell killing in the presence of the prodrug is specific or if the prodrug has a side effect of killing innocent cells. When 293T cells were transfected with pCMV-NTR-IRES-EGFP, the number of NTR expressing cells decreased at a 30 μM concentration (Figs. 2C and 2D). In fact, EGFP expressing cells were smaller and round but neighboring cells without EGFP expression maintained the intact morphology of cells (arrows in Fig. 2C), suggesting that there was no significant bystander killing at this concentration. Only EGFP$^+$ cell population in the 293T cells transfected with pCMV-NTR-IRES-EGFP showed annexin V staining (Table 1, Fig. 2E, and data not shown). EGFP$^-$ cells showed no binding of annexin V at the ranges of 10-30 μM prodrugs. Neither the DMSO treated pCMV-NTR-IRES-EGFP transfected cells nor cells transfected with pEGFP-N1 showed a sign of non NTR-associated cell death (data not shown). Treatment of MTZ at the same concentration also showed little bystander killing activity (data not shown). These data indicate that bystander killing of the non-NTR-producing cells by the prodrug treatment is insignificant under the condition that we tested. Together, we verified that MTZ and NFT specifically ablated NTR expressing cells *in vitro* and that two prodrugs are effective in inducing cell ablation.

Ablation of TEC in 3.1T-NE and 9.1T-NE transgenic fetal thymus

In order to identify the type of cells expressing EGFP, thymuses were treated with 2-dGuo for 1 week to deplete hematopoietic cells and cell suspensions were prepared from the culture to examine TEC subsets using flow cytometry (Fig. 3A). As shown in Fig. 3B, the pan epithelial marker EpCAM separated the population into 4 groups. After analyzing various combinations for the separation of a distinctive TEC population, we decided to include autofluorescence for the first gate along with EpCAM since it gave the best separation for EGFP expression. Then, 4 separate populations (S1-S4) were further divided into 7 separate subsets (S1, S2a, S2b, S3a, S3b, S4a, and S4b) based on the levels of EpCAM, MHCII, and CDR1 as well as EGFP ex-

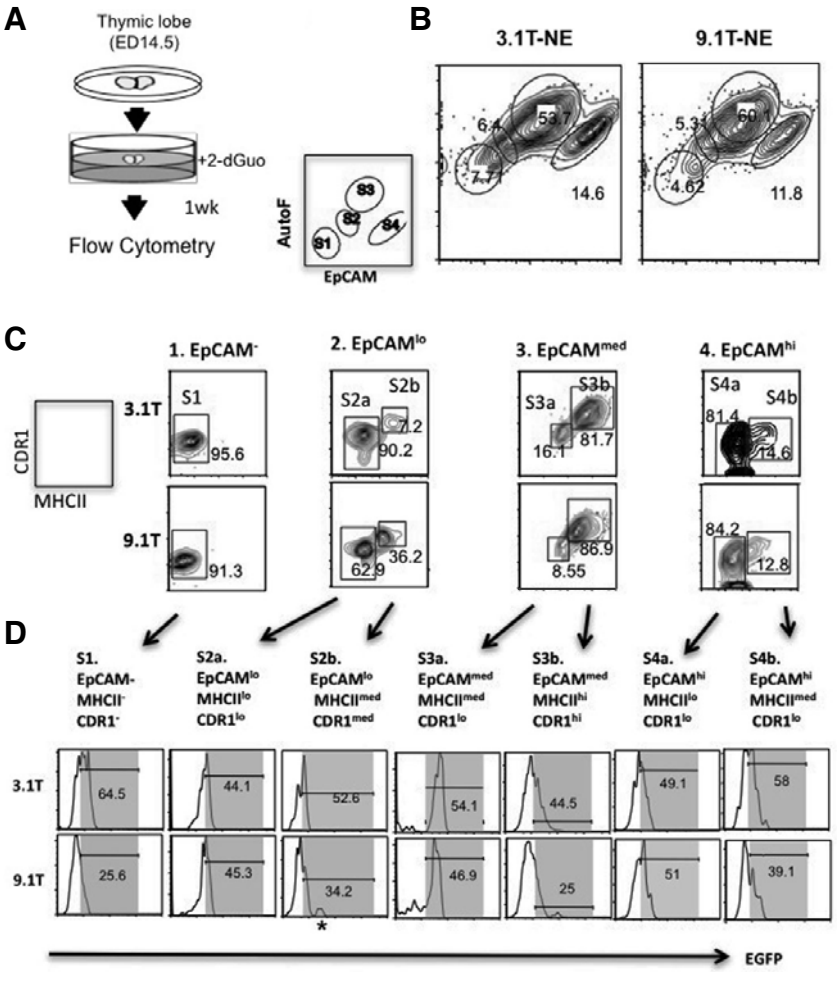

Fig. 3. Expression of EGFP in fetal TEC compartment of 3.1T-NE and 9.1T-NE transgenic mice. (A) Schematic presentation of the procedure for the detection of EGFP expression. (B) Profiles of TEC preparation in flow cytometry. EpCAM and autofluorescence profiles are shown. Four different subpopulations are indicated. (C) Division into 7 subsets using CDR1 and MHCII in addition to EpCAM (4 populations). (D) EGFP profiles of 7 subsets based on the levels of EpCAM, CDR1 and MHCII. EGFP expression in 7 TEC subsets of 3.1T-NE and 9.1T-NE are shown. Percentages of EGFP$^+$ gates are shown in the histogram.

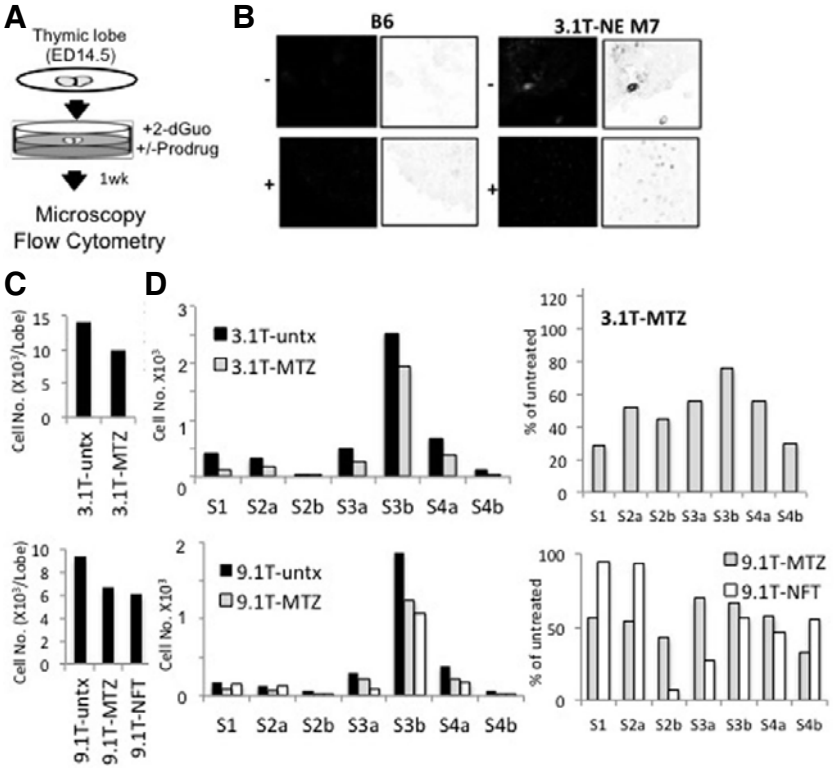

Fig. 4. Depletion of NTR and EGFP expressing TEC from FTOC with prodrugs MTZ and NFT. (A) Schematic presentation of experimental procedures. (B) Confocal microscopy of 2-dGuo and prodrug treated fetal thymus expressing NTR and EGFP. C57BL/6 (B6) on the left and 3.1T-NE (M7) are shown on the right. Upper panel shows the EGFP expressing patterns of thymic rudiment with 2d-Guo without prodrug; lower panel shows the EGFP expressing patterns of thymic rudiment with 2d-Guo and prodrug, 30 μM MTZ during FTOC of 3.1T-NE. Stylized patterns of EGFP expression are shown on the right. (C) Total stromal cell recovered (per lobe) after 3.1T-NE and of 9.1T-NE FTOC with prodrugs, MTZ and NFT at 30 μM in the presence of 2d-Guo. FTOCs were set with at least 14 lobes per group. (D) Numbers recovered (left) and % relative recovery to untreated samples (right) of seven TEC subsets described in Fig. 3 after FTOC of 3.1T-NE (top) and of 9.1T-NE (bottom) with prodrug treatments.

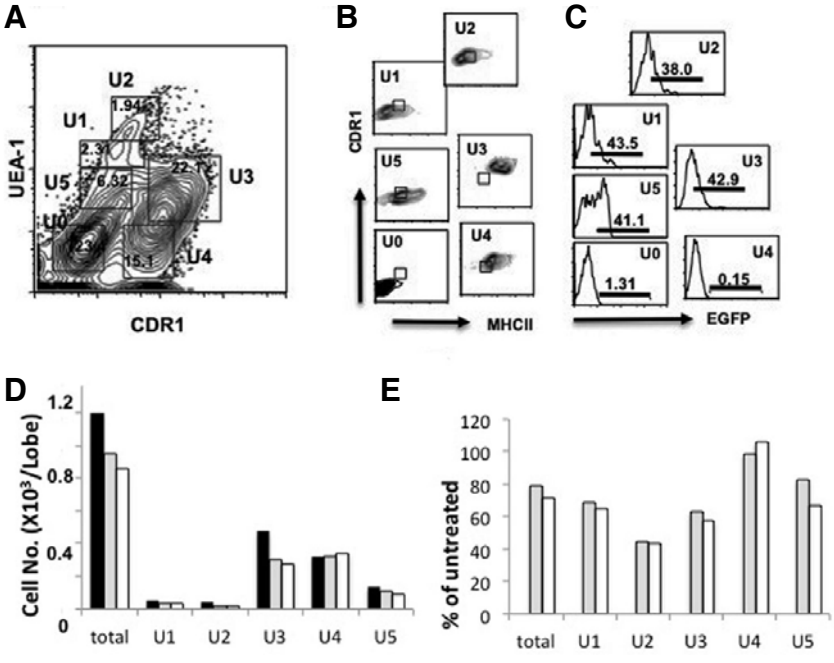

Fig. 5. Analysis of 9.1T-NE TEC with UEA-1 marker after prodrug induced depletion. (A) Representative profile of untreated TEC population. PI gated samples were displayed with CDR-1 and UEA-1. The 6 subsets separable (U0-U5) are shown in boxes. (B) MHCII and CDR1 profiles of each subset. The relative position for S2b of Fig. 3 is shown as small boxes in the profiles. (C) EGFP expression profiles of U0-U5 subsets. Percentages of the positive subsets are shown in numbers. (D) The numbers of TEC subsets recovered. DMSO treated (filled), MTZ treated (gray), and NFT treated (white) are shown. Total and U1-U5 subset are shown. (E) The relative percentages of treated samples to untreated samples. MTZ treated (gray) and NFT treated (white) are shown in percentages.

pression levels (Fig. 3D). In contrast to the location of specific compartments in adult thymus, both transgenic lines (3.1T-NE and 9.1T-NE) showed no distinctively separable populations; presumably both promoters are active in the overlapping population and at the precursor stages of TEC development. The negative control profiles for the EGFP expression derived from the nontransgenic thymus were variable among the TEC subsets (data not shown). In addition, transgenic EGFP profiles showed significant overlap in the cases of the lower EGFP expression as expected. Nonetheless, we carefully located the positive gates by considering the shapes of the histogram profiles that can be most separable from the negative profiles.

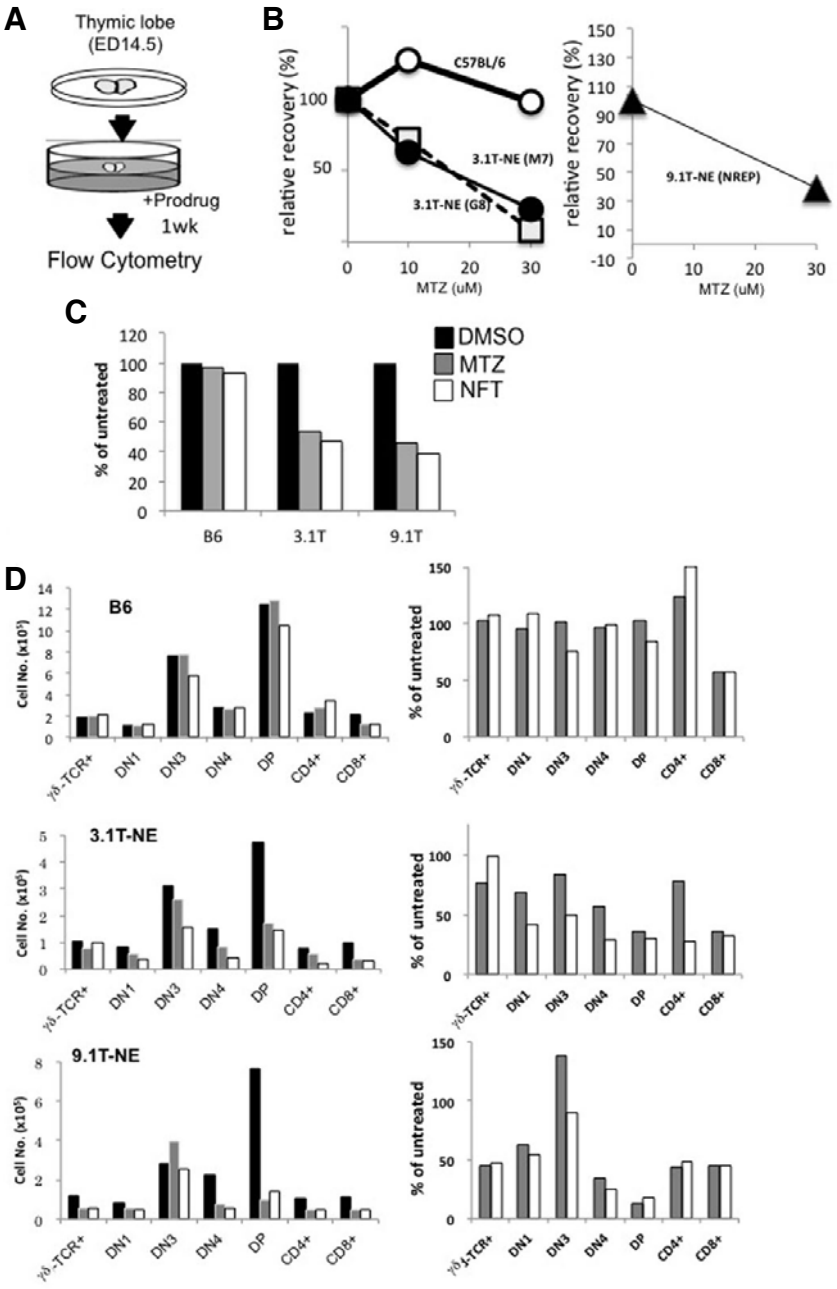

Fig. 6. Representative analysis of thymocyte development in the presence of prodrugs during FTOC. (A) Schematic presentation of experimental procedures. (B) Relative recovery (percentage) of the treated samples to the untreated samples. C57BL/6 (white circle), 3.1T-NE, G8 founder (black square), 3.1T-NE, M7 founder (gray square) are shown with indicated concentration of NFT. The line graph of 9.1T-NE with MTZ treatment is shown on the right. (C) Total thymocyte yields of FTOC of C57BL/6 (B6, n = 9 thymus/group), 3.1T-NE G8 (3.1T, n = 9 thymus/group) or 9.1T-NE NREP (9.1T, n = 10 thymus/group) treated with DMSO (Black) treated with 30 μM MTZ (gray) or 30 μM NFT (white). (D) Absolute numbers (left) and relative recovery (right) of each thymocyte compartments from FTOC in the presence of prodrugs. γδ T, DNs, DP, CD4, and CD8 cell patterns are shown. Top, C57BL/6 (B6), middle, 3.1T-NE, bottom, 9.1T-NE. DMSO (Black) treated with 30 μM MTZ (Gray) or 30 μM NFT (white). Data shown were obtained in the single experiment of whole sets that performed at the same time to avoid variations in the numbers.

Overall 3.1T-NE showed more EGFP^{+} cells in S1, S2b, S3b, and S4b subsets. A noticeable qualitative difference between 3.1T-NE and 9.1T-NE was located in subset S2b that was EpCAM^{lo}CDR1^{med}MHCII^{med}. EGFP^{high} expressor was found only in 9.1T-NE TEC population (marked with *). While 3.1T-NE showed no EGFP^{high} expression, 9.1T-NE showed 6.17% EGFP expressing cells. The presence of EGFP^{high} cells in the S2b subset appeared reproducible only in 9.1T-NE. These results indicate that thymic epithelial cells prepared from 2-dGuo treated fetal thymus are a heterogeneous mixture that can be divided into more distinct subsets using the *TSCOT* promoter activity along with EpCAM, MHCII, and CDR1. At this point, although it is difficult to assign these fetal TEC subsets to any specific TEC lineages, CDR1^{high} subsets are more likely to be the cTEC committed cells since CDR1 is a cTEC specific marker.

We next examined TEC ablation in FTOCs by treating the culture with prodrugs in the presence of 2d-Guo (Fig. 4A). Figure 4B shows EGFP expression patterns in the resulting thymic rudiments from 3.1T-NE transgenic thymuses. EGFP signals detectable in the E14.5 fetal thymus disappeared after treatment of prodrug MTZ for a week, while nontransgenic C57BL/6 did not show any sign of green fluorescence. The degree of depletion of EGFP expressing cells was further examined by flow cytometric analysis. As seen in Fig. 4C, the overall recoveries of total cell numbers from thymic rudiments (n = 14 each group) with 30 μM MTZ were about 60-70%. Despite a poor recovery of the cells, the degree of depletion in each subset of

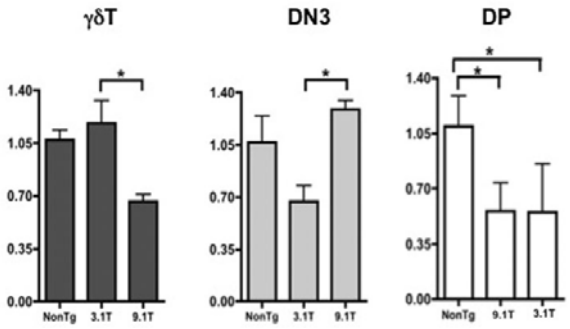

Fig. 7. The relative percentage of thymocyte subsets recovered from prodrug treatment. The average and standard error of means for the relative recoveries of γδT, DN3, and DP population were selected to show in the display. Statistical analyses were carried out using software Prism 4. One-way analyses of variance with the means showed significant differences. $P < 0.05$ for γδT and of DN3 between 3.1T-NE and 9.1T-NE and for DP between NonTg and 9.1T-NE and between NonTg and 3.1T-NE of by the Multiple Comparison Tests are shown. Data points (7-14) were obtained from the variable numbers of experiments.

3.1T-NE TEC population was in agreement with the relative proportion of $EGFP^+$ cells shown in Fig. 3D. Among all subsets, S1 and S4b subsets were highly susceptible showing 64.5% and 58% EGFP expressing cells, respectively (Fig. 3D). Treatment of 30 μM MTZ or NFT in 9.1T-NE thymuses also yielded reductions in all the subsets, particularly in S2b, S3a and S4b.

We further verified the depletion of TEC in 9.1T-NE using UEA-1 binding together with CDR-1 and MHCII. Previously, UEA-1 has been considered as a mTEC specific marker but the appearance of UEA-1 binding has not been clearly established in the fetal thymus. Analysis of UEA-1 and CDR1 revealed two small but distinct subsets, U1 ($UEA\text{-}1^{med}$, $MHCII^{lo}$, $CDR1^{lo}$) and U2 ($UEA\text{-}1^{high}$, $MHCII^{med}$, $CDR1^{med}$) (Fig. 5A). It is possible that these two populations may be precursor cells since they do not express high levels of MHCII. Alternatively, they may be the cells committed to the mTEC lineage. The profiles for EpCAM, MHCII, and CDR1 of the same cells revealed that the U2 subset overlaps with the S2b subset, $MHCII^{med}$, and $CDR1^{med}$ (Fig. 3). Major CDR1 expressing population was divided into 2 populations by the different levels of MHCII and EGFP expression (U3 and U4). In addition, the U5 subset was identified by a unique pattern of MHCII and high EGFP levels. Using the subset gates, depletion of each subset with MTZ and NFT prodrugs was shown in Figs. 5D and 5E. One of the major populations, CDR1 expressing U4 subset without EGFP expression did not show any sign of depletion, indicating little non-specific killing. Interestingly, the U2 subset was depleted most severely in 9.1T-NE stroma. Together with results from Fig. 4, subsets S2b and U2, both of which contain the same types of cells, ($EpCAM^{lo}CDR1^{med}MHCII^{med}UEA1^{hi}$) were depleted most. Although the absolute numbers were small in each subset, a similar pattern of EGFP expression and the degree of depletion with prodrug treatments indicate that we can achieve specific depletion of TEC using the inducible system.

Effect of TEC ablation on thymocyte development

After establishing the efficacy of the inducible cell ablation system, we investigated the effect of TEC depletion on thymocyte development. To do this, we set up a FTOC from two founder lines of 3.1T-NE (M7 and G8) and treated them with increasing doses of MTZ up to 30 μM. Results showed the dose dependent reduction in the recovery of total thymocyte numbers in the culture of 3.1T-NE not C57BL/6, suggesting that NTR independent nonspecific toxicity was minimum (Figs. 6B and 6C). The results from two founder lines of 3.1T-NE were indistinguishable (data not shown) and therefore we focused on the G8 founder line for 3.1T-NE and NREP for 9.1T-NE for subsequent experiments. The average of total thymocyte recovery of MTZ prodrug treated 9.1T-NE FTOC was 39.1+/-3.67% of DMSO treated 9.1T-NE FTOC (Fig. 6B on the right).

Next, we set up a large scale time pregnancy using normal and two transgenic lines (40-60 females per group) for a single experiment. Total thymocyte recoveries from the FTOC of C57BL/6, transgenic 3.1T-NE and 9.1T-NE were compared after treating cultures with MTZ or NFT at 30 μM. Neither prodrug treatments showed a toxic effect in C57BL/6, whereas the treatments clearly induced NTR-dependent killing in the FTOCs of 3.1T-NE and 9.1T-NE (Fig. 6C). There were noticeable variations in the absolute numbers (per lobe) recovered from untreated cultures among the strains (Fig. 6D). However, a comparison of the percentages of total thymocyte recovery with and without treatments showed a clear effect only in transgenic FTOCs.

As shown in Fig. 6D, the relative recoveries of γδ T cells, DN1, DN4, DP, and CD4 cells from C57BL/6 showed little interference by the presence of prodrugs in FTOC. Neither MTZ nor NFT seemed to have the nonspecific toxicity in those cell populations. The only deviation with an unknown reason resided in the CD8 population. Inclusion of prodrugs in the FTOC showed a severe reduction in DN4, DP, and CD4 population in both transgenic 3.1T-NE and 9.1T-NE. Although the general patterns of two transgenic lines were similar, the recovery of γδ T cells and DN3 was different between the two transgenic lines. As summarized in Fig. 7, the relative recovery of γδ T cells was clearly diminished in the 9.1T-NE FTOC, whereas DN3 cells were reduced in the 3.1T-NE line. The recoveries of absolute numbers of DP cells showed significant and comparable reductions in both lines.

In conclusion, TEC depletion of the transgenic thymus with prodrugs resulted in a reduction of thymocyte recovery for the mainstream αβ T cell lineages in both transgenic lines, but the effects during the earlier developmental stages were different. Interference by NTR-mediated TEC depletion for DN3 was restricted in 3.1T-NE, while that for γδ T cells was noticeable only in 9.1T-NE.

Developmental stage and lineage specific roles of TEC subsets revealed by RTOC

When we set up a FTOC using 14.5 day old fetal thymuses, the culture contained thymocytes at DN2 and DN3 stages that already committed to αβ and γδ T cell lineages. Therefore, the thymocyte population in the FTOC is a mixture of cells at various developmental stages to begin with. To have a better assessment of the role of the TEC subset for thymocyte development, we employed a RTOC with E14.5 fetal liver progenitor cells. We prepared the TEC in the presence of 2d-Guo, aggregated it with E14.5 fetal liver progenitor cells, and analyzed cells 7 days later (Fig. 8A). Thymocytes from the RTOC consisted mostly of DN cells (50.9%). The γδ T cells were more abundant in RTOC (4.86%) compared to that in adults (0.96%). DN subpopulations in the RTOC were clearly separated into DN1-DN3 using CD44 and CD25 profiles. A small fraction of the DN population in the RTOC was of $Sca1^+cKit^+$ cells.

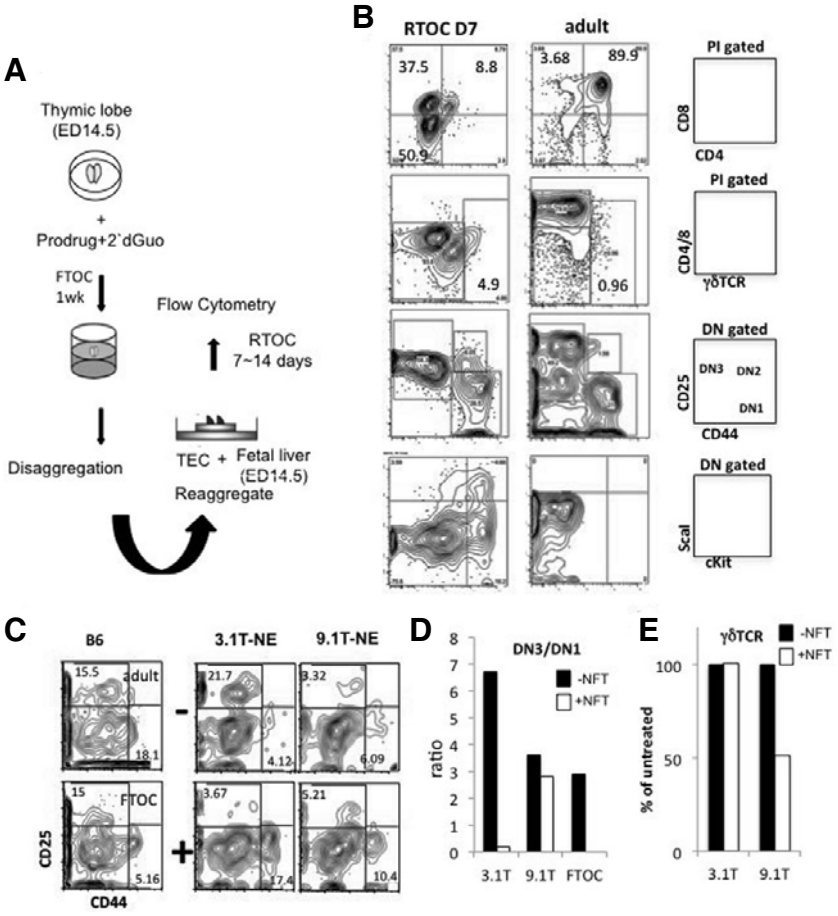

Fig. 8. Analysis of thymocytes recovered from RTOC of fetal liver progenitor cells and TEC preparation depleted with prodrugs. (A) General scheme of RTOC with NTR mediated TEC depletion. (B) Gates of thymocyte population recovered from RTOC (left) at day 7 and those of adult thymocytes (middle). Each parameter and all gates are indicated (right). (C) CD44 and CD25 profiles of DN cells from RTOC at day 9 of fetal liver and TEC preparation without (-) and with (+) treatment of 30 μM NFT during initial FTOC with 2-dGuo. The profiles of normal adult thymus and of normal FTOC are shown on the left (B6). Names of mouse lines are shown on top. (D) The ratios of DN3/DN1 in RTOC. Untreated TEC (black) treated TEC (white). (E) Percentage γδ T cells recovered. RTOC with untreated TEC (black) and that of treated TEC (white).

Next, we examined the effect of TEC ablation using the same strategy for the FTOC. When the RTOC was analyzed at day 9, non-transgenic C57BL/6 stroma showed no significant difference for the DN profiles upon the prodrug treatment (Fig. 8C and data not shown). However, the DN profiles changed in 3.1T-NE and 9.1T-NE transgenic RTOCs. We calculated the ratio of DN3/DN1 without including DN2 since the cell numbers in the DN2 population were too low to obtain an accurate measurement. The ratio of DN3/DN1 of 3.1T-NE was greatly diminished. In contrast, the DN3/DN1 ratio of 9.1T-NE RTOC was comparable with and without prodrug treatment (Fig. 8D).

The levels were also similar to that of the FTOC with non-transgenic C57BL/6 thymus, indicating that transition from DN1 to DN3 was not affected in 9.1T-NE. In regards to the recovery however, γδ T cells were greatly reduced in 9.1T-NE but not in the 3.1T-NE RTOC (Fig. 8E) consistent with the earlier results from the FTOC (Figs. 6 and 7).

We also examined the cell populations after 14 days of the RTOC and found a very poor recovery of the thymocytes in the RTOC with 9.1T-NE TEC preparation (Fig. 9A). The total numbers and relative recovery of DN and γδ T cells were also severely reduced in the 9.1T-NE RTOC (Fig. 9B and data not shown). Interestingly, there was an opposing effect of TEC depletion on the DN3/DN1 ratio and γδ T cells between two lines of mice. The γδ T cell development was dramatically reduced in 9.1T-NE, whereas 3.1T-NE showed a reduction in the DN3/DN1 ratio but not γδ T cells (Figs. 9C and 9D). However, flow cytometric profiles showed a relatively good DN3/DN1 ratio with or without the prodrug treatment in TEC preparation of 9.1T-NE. The RTOC with depleted 3.1T-NE showed consistently low DN3/DN1 ratios upon prodrug treatment, and 9.1T-NE showed abrogation of γδ T cells. These results are consistent with the results from the FTOC and the RTOC at day 9, supporting the idea of lineage and stage specific roles of TEC.

DISCUSSION

In this study we introduced two inducible TEC ablation systems using NTR and the prodrugs, MTZ and NFT. Two sizes of the *TSCOT* promoter in the transgene drove reporter gene expression in TEC with minor differences that are distinguished based on the potential of TEC to support γδ T and DN cell differentiation tested by FTOC and RTOC.

Suicide gene approach with NTR enzyme and alternative prodrugs, MTZ and NFT

Use of suicide genes has been employed for research and cancer gene therapy (Dachs et al., 1997; Lal et al., 2000; Yazawa et al., 2002). Most suicide genes utilize DNA metabolism and therefore, only dividing cells can be targeted. NTR, on the other hand, is an enzyme which produces a toxic product that can modify DNA regardless of the cell cycle. Since thymic stromal cells are rather static and many of them are not in any cycle, NTR seems to be an excellent reagent to induce death of

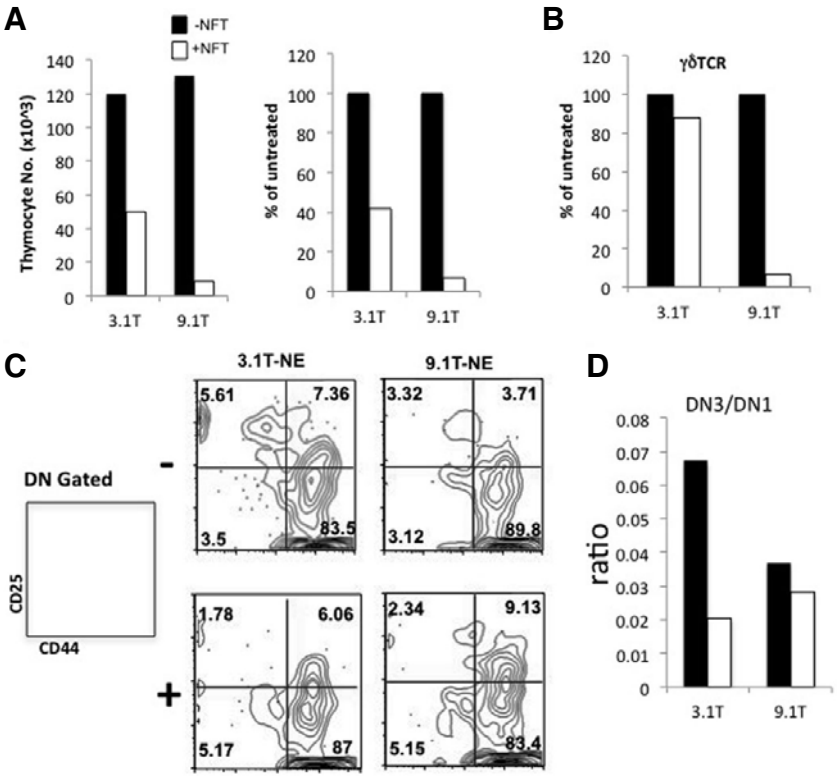

Fig. 9. Analysis of RTOC at day 14 of fetal liver and depleted TEC treated with prodrugs. (A) Total thymocyte yields of RTOC of 3.1T-NE and 9.1T-NE with or without NTR mediated ablation of TEC. Relative recovery of total thymocyte of RTOC of 3.1T-NE and 9.1T-NE are shown on the right. (B) Relative yield of γδ T cells from RTOC. (C) Profiles of CD44 and CD25 (DN gate) RTOC with TEC without depletion (-) and with depletion (+). (D) The ratios of DN3/DN1 from RTOC of 3.1T-NE and 9.1T-NE TEC. The black bar indicates results without the depletion and the white bar indicates results with the depletion.

TEC. Although NTR has been previously applied in transgenic mouse and cancer gene therapy model (Bailey et al., 1996; Laufer et al., 1999), most of the NTR applications in those cases used prodrug CB1954 (Bailey and Hart, 1997). In fact, CB1954 is useful in cancer therapy because it generates significant bystander killing. However, MTZ and NFT have an advantage over CB1954. MTZ and NFT are readily available and, more importantly, they showed apoptotic cell death with little bystander killing as we demonstrated (Figs. 2 and 6).

TSCOT promoter activity during thymic compartmentalization

TSCOT is a unique gene that is expressed in the thymic cortex (Ahn et al., 2008; Kim et al., 2000a; Yang et al., 2005). Other than *TSCOT,* there are a small number of genes known to be expressed in the thymic cortex (Bowlus et al., 1999; Kirchner et al., 2001; Murata et al., 2007; Tomaru et al., 2009). Although these gene expressions are compartmentalized into the thymic cortex and some of the gene products are known for their functions, the mechanisms of the gene expression and the roles for the specific TEC compartmentalization still remain as questions. Here, we showed that different lengths of the *TSCOT* promoter are active in the different compartments, while the endogenous gene is active in the thymic cortex. When a *lacZ* reporter gene was targeted into the *TSCOT* locus (Ahn et al., 2008) or a 9.1 kb *TSCOT* promoter was used to direct EGFP expression (Fig. 1C), both reporters were expressed in the cortical area of the adult thymus. However, when a 3.1 kb *TSCOT* promoter was used, expression appeared in the medulla (Fig. 1C and unpublished results). Therefore, it is reasonable to assume that compartment specific *cis* and *trans* regulatory elements are present in each promoter, which then directs gene expression in the cortex during the differentiation and compartmentalization of TEC. In the analysis of evolutionary conservation of promoter sequences, we found that there are more conserved areas upstream of the 3.1 kb promoter (Chen et al., 2000).

Based on EGFP expression along with EpCAM, MHCII and CDR1 in the thymic stromal cells from the FTOC treated with 2d-Guo of 3.1T-NE and 9.1T-NE, TEC compartments were further divided into $9.1T^+$ TEC and/or $3.1T^+$ TEC. Distinctive populations found in this study are as follow: subset S1, $EpCAM^-MHCII^-CDR1^-$ (nonTEC), subset S2a, $EpCAM^{lo}MHCII^{lo}CDR1^{lo}$, subset S2b $EpCAM^{lo}MHCII^{med}CDR1^{med}$, subset S3a $EpCAM^{med}MHCII^{med}CDR1^{lo}$, subset S3b $EpCAM^{med}MHCII^{hi}CDR1^{hi}$, subset S4a $EpCAM^{med}MHCII^{lo}CDR1^{lo}$, subset S4b $EpCAM^{hi}MHCII^{med}CDR1^{lo}$ (some are $EGFP^-$). Subset 2b is particularly interesting since there is no EGFP high expresser in 3.1T-NE thymus but it is present in 9.1T-NE. This subset appeared to include cells expressing the medullary marker UEA-1 (U2 in Fig. 5) and was depleted most severely in 9.1T-NE (Figs. 6-8). It is not clear if this subset is lineage committed or not since UEA-1 is considered as a good medullary marker but the adult thymus of 9.1T-NE maintained cortical expression. Regardless, it is interesting that this population includes TEC subsets that support γδ T cell development.

The 3.1T-NE thymus contained more EGFP expressing cells than 9.1T-NE thymus and expressed EGFP in medulla and CMJ in adults (Fig. 1C). Since it is usually considered fetal thymus does not have a fully differentiated mTEC compartment, it is possible that subsets S3b (both express cTEC marker CDR1 at low levels as well as MHCII at the medium levels) contain a precursor population for mTEC or a common precursor, pTEC for both cTEC and mTEC.

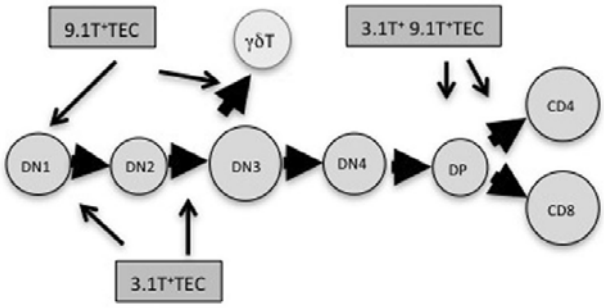

Fig. 10. Model of thymocyte lineage choice and stage specific progression regulated with specific TEC subsets. Thymocyte populations are shown in circles, TEC are shown in rectangles. Allocation of TEC subsets was based on the EGFP expression, depletion, and the results of FTOC and RTOC. Thick arrows indicate the direction of differentiation; thin arrows indicate the stages for the putative roles of specific TEC population.

Studies of ontogeny and differentiation of cTEC during fetal stages showed that expression levels of the marker and the percentages of marker expressing cells are not static but are dynamic (Shakib et al., 2009; Yang et al., 2005; 2006). Our results also showed dynamic and complex populations in the fetal thymus. Detailed analysis on cTEC and mTEC development still remains to be investigated further.

Role of specific TEC populations in the progression and the lineage choice of T cells

A model summarizing the current work is presented in Fig. 10. FTOC and RTOC combined with specific TEC depletion showed that DP and CD4 SP development was severely affected in both transgenic lines (Figs. 6 and 7). DP and CD4 SP cells depend on cTEC that was depleted in both the 3.1T-NE and 9.1T-NE thymus for their selection. Therefore it is not surprising that depletion of major fetal MHCII expressing TEC failed to support the survival of thymocytes in culture. Massive cell death in the DP population by the lack of the appropriate type and/or insufficient numbers of cTEC is most likely due to the lack of positive selection, resulting in death by neglect. The BJ Fowlkes group showed the effects of the thymic microenvironment on MHCII specific thymocyte selection by using mixed chimeras of selectable and non-selectable thymocytes with the same specificity (Canelles et al., 2003). They also showed segregated compartments are present for the selection of CD4 or CD8 SP cells in the thymus. Therefore, each compartment in the cortical microenvironment seems to possess a distinctive function to support the development of thymocytes with a different fate.

It was surprising to find that TEC depleted in 3.1T-NE and 9.1T-NE mediate early T cell development differently. There was a blockade before DN3 in RTOC with depleted 3.1T-NE TEC, whereas γδ T cell development was poor in RTOC with depleted 9.1T-NE TEC (Figs. 6-9). These results strongly support the idea that a separate population of thymic stromal cells supports the thymocyte lineage choice and the checkpoints for the stage specific thymic development. S2b/U2 subsets that include UEA-1$^+$ EGFP$^+$ cells (also for CDR^{med} and MHCII^{med}) are good candidates that support γδ T cell development since it is depleted more severely in 9.1T-NE than 3.1T-NE (Figs. 4 and 5). Since Graham Anderson's group showed Vγ5$^+$ T cells depend on AIRE$^+$ TEC (Roberts et al., 2012), it will be interesting to see if the S2b/U2 population contains the AIRE expressing cells. The expression of the mTEC marker UEA-1 in this population supports the notion that this subset is not of conventional cTEC committed cells.

It is interesting to see the clear difference in the ratios of DN3/DN1 with specific depletion of TEC from 3.1T-NE and 9.1T-NE. Previously, we showed that laminin 5 expressed in the subset of fetal TEC is responsible for the survival of DN3 (Kim et al., 2000b). DN3 cells depend on laminin 5 present on TEC subsets and die by anchorage dependent apoptosis (anoikis) if interaction to laminin 5 is absent. In FTOC and RTOC with depleted TEC from 3.1T-NE, the DN3 population was distinctively reduced in numbers. This abrogation of DN3 in RTOC with depleted 3.1T-NE stroma may be due to increased apoptosis or anoikis rather than a developmental defect.

IL-7 is an important cytokine for the survival of early thymocytes (Alves et al., 2010; Balciunaite et al., 2005) as well as thymocytes undergoing selection (Park et al., 2004; 2010) and critical for the development of γδ T cells (Moore et al., 1996). In the absence of IL-7, all the γδ T cell development, including fetal γδ T cells, is severely affected. In an earlier work, by using RTOC of a fetal liver progenitor and with thymic stromas from the various mutant mouse lines (Oosterwegel et al., 1997), it was shown that IL-7 producing MHCII$^+$ TEC cells are important for the rearrangement of β and δ loci of CD117$^+$CD45$^+$ fetal liver progenitors. IL-7 producing TECs are noticed in early thymic organogenesis, and even nude thymic rudiments demonstrate the message expression (Zamisch et al., 2005). In later stages, IL-7 expression is located in the cortical area (Alves et al., 2010). This expression profile is consistent with that of *TSCOT*.

An immunoglobulin superfamily protein, Skint-1 was identified as an essential protein expressed in TEC for the development of Vγ5Vδ1T cells (Barbee et al., 2011; Boyden et al., 2008). In addition, RANK signaling was found to be critical for developing the same cells. These results provide evidence for the presence of a unique pathway of the γδ T cell development at the molecular level. There were also significant data that the Notch pathway is involved in the decision for αβ vs. γδ T cell lineage as well as other fate decisions during T cell development (Laky and Fowlkes, 2008; Laky et al., 2006). However, questions for the existence of a role for specific notch ligands in TEC function is still open.

Although 3.1T-NE and 9.1T-NE thymus revealed only small differences in the populations expressing EGFP (Figs. 3-5), the effect of TEC depletion resulted in different T cell development profiles. Therefore, it is clear that the TEC population mediating DN1 to DN3 progression, and that for γδ T cell development, are distinctly different. Perhaps these TEC subsets may express different ligands. However, it is still a challenge to find the detailed expression profile of molecules in specific TEC cells by conventional gene expression analysis.

ACKNOWLEDGMENTS

We thank Dr. Ronald Schwartz in the NIH for the support during the early stage of this work, and Mincheol Kim and Jenifer Westrup for their technical help. We greatly appreciate Drs. Leinol Fagenbaum and Han-Woong Lee for the generation and maintenance of the mice, Dr. Owen Schwartz for the help in confocal microscopy, and Dr. Larry Lantz for the production of critical antibodies. This work was supported by the Mid-career Researcher Program (E00023, 2009-0080621) of the National Research Foundation grant funded by the Ministry of Education, Science and Technology, Korea and Inha University Research Grant.

REFERENCES

Ahn, S., Lee, G., Yang, S.J., Lee, D., Lee, S., Shin, H.S., Kim, M.C., Lee, K.N., Palmer, D.C., Theoret, M.R., et al. (2008). TSCOT+ thymic epithelial cell-mediated sensitive CD4 tolerance by direct presentation. PLoS Biol. *6*, e191.

Alves, N.L., Huntington, N.D., Mention, J.J., Richard-Le Goff, O., and Di Santo, J.P. (2010). Cutting edge: a thymocyte-thymic epithelial cell cross-talk dynamically regulates intrathymic IL-7 expression *in vivo*. J. Immunol. *184*, 5949-5953.

Anderson, G., and Jenkinson, E.J. (2007). Fetal thymus organ culture. CSH Protoc. *2007*, pdb prot4808.

Anderson, G., Jenkinson, E.J., Moore, N.C., and Owen, J.J. (1993). MHC class II-positive epithelium and mesenchyme cells are both required for T-cell development in the thymus. Nature *362*, 70-73.

Anderson, G., Jenkinson, E.J., and Rodewald, H.R. (2009). A roadmap for thymic epithelial cell development. Eur J. Immunol. *39*, 1694-1699.

Anderson, G., and Takahama, Y. (2012). Thymic epithelial cells: working class heroes for T cell development and repertoire selection. Trends Immunol. *33*, 256-263.

Bailey, S.M., and Hart, I.R. (1997). Nitroreductase activation of CB1954--an alternative 'suicide' gene system. Gene Ther. *4*, 80-81.

Bailey, S.M., Knox, R.J., Hobbs, S.M., Jenkins, T.C., Mauger, A.B., Melton, R.G., Burke, P.J., Connors, T.A., and Hart, I.R. (1996). Investigation of alternative prodrugs for use with *E. coli* nitroreductase in 'suicide gene' approaches to cancer therapy. Gene Ther. *3*, 1143-1150.

Balciunaite, G., Ceredig, R., Fehling, H.J., Zuniga-Pflucker, J.C., and Rolink, A.G. (2005). The role of Notch and IL-7 signaling in early thymocyte proliferation and differentiation. Eur. J. Immunol. *35*, 1292-1300.

Barbee, S.D., Woodward, M.J., Turchinovich, G., Mention, J.J., Lewis, J.M., Boyden, L.M., Lifton, R.P., Tigelaar, R., and Hayday, A.C. (2011). Skint-1 is a highly specific, unique selecting component for epidermal T cells. Proc. Natl. Acad. Sci. USA *108*, 3330-3335.

Blackburn, C.C., and Manley, N.R. (2004). Developing a new paradigm for thymus organogenesis. Nat. Rev. Immunol. *4*, 278-289.

Bowlus, C.L., Ahn, J., Chu, T., and Gruen, J.R. (1999). Cloning of a novel MHC-encoded serine peptidase highly expressed by cortical epithelial cells of the thymus. Cell Immunol. *196*, 80-86.

Boyden, L.M., Lewis, J.M., Barbee, S.D., Bas, A., Girardi, M., Hayday, A.C., Tigelaar, R.E., and Lifton, R.P. (2008). Skint1, the prototype of a newly identified immunoglobulin superfamily gene cluster, positively selects epidermal gammadelta T cells. Nat. Genet. *40*, 656-662.

Bridgewater, J.A., Knox, R.J., Pitts, J.D., Collins, M.K., and Springer, C.J. (1997). The bystander effect of the nitroreductase/CB1954 enzyme/prodrug system is due to a cell-permeable metabolite. Hum. Gene Ther. *8*, 709-717.

Cahill, R.N., Kimpton, W.G., Washington, E.A., Holder, J.E., and Cunningham, C.P. (1999). The ontogeny of T cell recirculation during foetal life. Semin. Immunol. *11*, 105-114.

Canelles, M., Park, M.L., Schwartz, O.M., and Fowlkes, B.J. (2003) The influence of the thymic environment on the CD4-versus-CD8 T lineage decision. Nat. Immunol. *4*, 756-764.

Chen, C., Kim, M.G., Soo Lyu, M., Kozak, C.A., Schwartz, R.H., and Flomerfelt, F.A. (2000). Characterization of the mouse gene, human promoter and human cDNA of TSCOT reveals strong interspecies homology. Biochim. Biophys. Acta *1493*, 159-169.

Ciofani, M., and Zuniga-Pflucker, J.C. (2010). Determining gammadelta versus alphas T cell development. Nat. Rev. Immunol. *10*, 657-663.

Crompton, T., Outram, S.V., and Hager-Theodorides, A.L. (2007). Sonic hedgehog signalling in T-cell development and activation. Nat. Rev. Immunol. *7*, 726-735.

Dachs, G.U., Dougherty, G.J., Stratford, I.J., and Chaplin, D.J. (1997). Targeting gene therapy to cancer: a review. Oncol. Res. *9*, 313-325.

Gray, D.H., Chidgey, A.P., and Boyd, R.L. (2002). Analysis of thymic stromal cell populations using flow cytometry. J. Immunol. Methods *260*, 15-28.

Gray, D.H., Seach, N., Ueno, T., Milton, M.K., Liston, A., Lew, A.M., Goodnow, C.C., and Boyd, R.L. (2006). Developmental kinetics, turnover, and stimulatory capacity of thymic epithelial cells. Blood *108*, 3777-3785.

Jenkinson, E.J., and Owen, J.J. (1990). T-cell differentiation in thymus organ cultures. Semin. Immunol. *2*, 51-58.

Jenkinson, E.J., and Anderson, G. (1994). Fetal thymic organ cultures. Curr. Opin. Immunol. *6*, 293-297.

Jo, D., Lyu, M.S., Cho, E.G., Park, D., Kozak, C.A., and Kim, M.G. (2001). Identification and genetic mapping of the mouse Fkbp9 gene encoding a new member of FK506-binding protein family. Mol. Cells *12*, 272-275.

Kim, M.G., Chen, C., Flomerfelt, F.A., Germain, R.N., and Schwartz, R.H. (1998). A subtractive PCR-based cDNA library made from fetal thymic stromal cells. J. Immunol. Methods *213*, 169-182.

Kim, M.G., Flomerfelt, F.A., Lee, K.N., Chen, C., and Schwartz, R.H. (2000a). A putative 12 transmembrane domain cotransporter expressed in thymic cortical epithelial cells. J. Immunol. *164*, 3185-3192.

Kim, M.G., Lee, G., Lee, S.K., Lolkema, M., Yim, J., Hong, S.H., and Schwartz, R.H. (2000b). Epithelial cell-specific laminin 5 is required for survival of early thymocytes. J. Immunol. *165*, 192-201.

Kirchner, J., Forbush, K.A., and Bevan, M.J. (2001). Identification and characterization of thymus LIM protein: targeted disruption reduces thymus cellularity. Mol. Cell. Biol. *21*, 8592-8604.

Ladi, E., Yin, X., Chtanova, T., and Robey, E.A. (2006). Thymic microenvironments for T cell differentiation and selection. Nat. Immunol. *7*, 338-343.

Laky, K., and Fowlkes, B.J. (2008). Notch signaling in CD4 and CD8 T cell development. Curr. Opin. Immunol. *20*, 197-202.

Laky, K., Fleischacker, C., and Fowlkes, B.J. (2006). TCR and Notch signaling in CD4 and CD8 T-cell development. Immunol. Rev. *209*, 274-283.

Lal, S., Lauer, U.M., Niethammer, D., Beck, J.F., and Schlegel, P.G. (2000). Suicide genes: past, present and future perspectives. Immunol. Today *21*, 48-54.

Laufer, T.M. (2008) Tolerance to self: which cells kill? PLoS Biol. *6*, e241.

Laufer, T.M., DeKoning, J., Markowitz, J.S., Lo, D., and Glimcher, L.H. (1996). Unopposed positive selection and autoreactivity in mice expressing class II MHC only on thymic cortex. Nature *383*, 81-85.

Laufer, T.M., Glimcher, L.H., and Lo, D. (1999). Using thymus anatomy to dissect T cell repertoire selection. Semin. Immunol. *11*, 65-70.

Lee, C., Kim, M.G., Jeon, S.H., Park, D.E., Park, S.D., and Seong, R.H. (1998). Two species of mRNAs for the fyn proto-oncogene are produced by an alternative polyadenylation. Mol. Cells *8*, 746-749.

Lee, G., Kim, M.G., Yim, J.B., and Hong, S.H. (2001). Alternative transcriptional initiation and splicing of mouse Lamc2 message. Mol. Cells *12*, 380-390.

Moore, T.A., von Freeden-Jeffry, U., Murray, R., and Zlotnik, A. (1996). Inhibition of gamma delta T cell development and early thymocyte maturation in IL-7 -/- mice. J. Immunol. *157*, 2366-2373.

Murata, S., Sasaki, K., Kishimoto, T., Niwa, S., Hayashi, H., Takahama, Y., and Tanaka, K. (2007). Regulation of CD8+ T cell development by thymus-specific proteasomes. Science *316*, 1349-1353.

Narayan, K., and Kang, J. (2007). Molecular events that regulate alphabeta versus gammadelta T cell lineage commitment: old suspects, new players and different game plans. Curr. Opin. Immunol. *19*, 169-175.

Oosterwegel, M.A., Haks, M.C., Jeffry, U., Murray, R., and Kruisbeek, A.M. (1997). Induction of TCR gene rearrangements in uncommitted stem cells by a subset of IL-7 producing, MHC class-II-expressing thymic stromal cells. Immunity *6*, 351-360.

Park, D. (1997). Cloning, sequencing, and overexpression of SH2/SH3 adaptor protein Nck from mouse thymus. Mol. Cells *7*, 231-236.

Park, J.H., Yu, Q., Erman, B., Appelbaum, J.S., Montoya-Durango, D., Grimes, H.L., and Singer, A. (2004). Suppression of IL7R alpha transcription by IL-7 and other prosurvival cytokines: a novel mechanism for maximizing IL-7-dependent T cell survival. Im-

munity *21*, 289-302.
Park, J.H., Adoro, S., Guinter, T., Erman, B., Alag, A.S., Catalfamo, M., Kimura, M.Y., Cui, Y., Lucas, P.J., Gress, R.E., et al. (2010). Signaling by intrathymic cytokines, not T cell antigen receptors, specifies CD8 lineage choice and promotes the differentiation of cytotoxic-lineage T cells. Nat. Immunol. *11*, 257-264.
Petrie, H.T. (2003). Cell migration and the control of post-natal T-cell lymphopoiesis in the thymus. Nat. Rev. Immunol. *3*, 859-866.
Petrie, H.T., and Zuniga-Pflucker, J.C. (2007). Zoned out: functional mapping of stromal signaling microenvironments in the thymus. Annu. Rev. Immunol. *25*, 649-679.
Roberts, N.A., White, A.J., Jenkinson, W.E., Turchinovich, G., Nakamura, K., Withers, D.R., McConnell, F.M., Desanti, G.E., Benezech, C., Parnell, S.M., et al. (2012). Rank signaling links the development of invariant gammadelta T cell progenitors and Aire(+) medullary epithelium. Immunity *36*, 427-437.
Rodewald, H.R. (2008).Thymus organogenesis. Annu. Rev. Immunol. *26*, 355-388.
Shakib, S., Desanti, G.E., Jenkinson, W.E., Parnell, S.M., Jenkinson, E.J., and Anderson, G. (2009). Checkpoints in the development of thymic cortical epithelial cells. J. Immunol. *182*, 130-137.
Takahama, Y. (2006). Journey through the thymus: stromal guides for T-cell development and selection. Nat. Rev. Immunol. *6*, 127-135.
Takahama, Y., Nitta, T., Mat Ripen, A., Nitta, S., Murata, S., and Tanaka, K. (2010). Role of thymic cortex-specific self-peptides in positive selection of T cells. Semin. Immunol. *22*, 287-293.
Tomaru, U., Ishizu, A., Murata, S., Miyatake, Y., Suzuki, S., Takahashi, S., Kazamaki, T., Ohara, J., Baba, T., Iwasaki, S., et al. (2009). Exclusive expression of proteasome subunit {beta}5t in the human thymic cortex. Blood *113*, 5186-5191.
White, A., Jenkinson, E., and Anderson, G. (2008). Reaggregate thymus cultures. J. Vis. Exp. *18*, 905.
Wong, G.W., and Zuniga-Pflucker, J.C. (2010). gammadelta and alphabeta T cell lineage choice: resolution by a stronger sense of being. Semin. Immunol. *22*, 228-236.
Yang, S.J., Ahn, S., Park, C.S., Choi, S., and Kim, M.G. (2005). Identifying subpopulations of thymic epithelial cells by flow cytometry using a new specific thymic epithelial marker, Ly110. J. Immunol. Methods *297*, 265-270.
Yang, S.J., Ahn, S., Park, C.S., Holmes, K.L., Westrup, J., Chang, C.H., and Kim, M.G. (2006). The quantitative assessment of MHC II on thymic epithelium: implications in cortical thymocyte development. Int. Immunol. *18*, 729-739.
Yazawa, K., Fisher, W.E., and Brunicardi, F.C. (2002). Current progress in suicide gene therapy for cancer. World J. Surg. *26*, 783-789.
Zamisch, M., Moore-Scott, B., Su, D.M., Lucas, P.J., Manley, N., and Richie, E.R. (2005). Ontogeny and regulation of IL-7-expressing thymic epithelial cells. J. Immunol. *174*, 60-67.